Molecular Therapy
Original Article

Targeted Allele Suppression Prevents Progressive Hearing Loss in the Mature Murine Model of Human *TMC1* Deafness

Hidekane Yoshimura,[1,2] Seiji B. Shibata,[1,3] Paul T. Ranum,[1] Hideaki Moteki,[2] and Richard J.H. Smith[1,3]

[1]Molecular Otolaryngology and Renal Research Laboratories, Carver College of Medicine, University of Iowa, Iowa City, IA 52242, USA; [2]Department of Otorhinolaryngology, Shinshu University School of Medicine, Matsumoto, Nagano 390-8621, Japan; [3]Department of Otolaryngology-Head and Neck Surgery, Carver College of Medicine, University of Iowa, Iowa City, IA 52242, USA

Hearing loss is the most common human sensory deficit. Its correction has been the goal of several gene-therapy based studies exploring a variety of interventions. Although these studies report varying degrees of success, all treatments have targeted developing inner ears in neonatal mice, a time point in the structural maturation of the cochlea prior to 26 weeks gestational age in humans. It is unclear whether cochlear gene therapy can salvage hearing in the mature organ of Corti. Herein, we report the first study to test gene therapy in an adult murine model of human deafness. Using a single intracochlear injection of an artificial microRNA carried in an AAV vector, we show that RNAi-mediated gene silencing can slow progression of hearing loss, improve inner hair cell survival, and prevent stereocilia bundle degeneration in the mature *Beethoven* mouse, a model of human *TMC1* deafness. The ability to study gene therapy in mature murine ears constitutes a significant step toward its translation to human subjects.

INTRODUCTION

Hearing loss (HL) is the most common sensory deficit in humans. In approximately 360 million people worldwide it profoundly impacts quality of life by causing social isolation, economic disadvantage, and stigmatization. In the young, it leads to delayed speech development and carries an estimated lifetime cost in excess of $1 million.[1] Current treatment options include hearing amplification and cochlear implantation.[2] Although both interventions are effective, neither restores natural hearing. As the hearing-impaired population is expected to increase over the next decade, novel therapeutics capable of treating the mature auditory system are an important goal toward enhancing quality of life.

In earlier work, we investigated the effect of RNAi-based gene therapy in the neonatal *Beethoven* (*Bth*) mouse, a murine model of human *TMC1* deafness (DFNA36 [MIM: 606705]). *Bth* mice carry a dominant-negative missense mutation, c.1235T > A (p.Met412Lys), in the transmembrane channel-like gene 1 (*Tmc1*) gene[3] that is orthologous to the c.1253T > A (p.Met418Lys) variant reported in human *TMC1* in two Chinese families segregating early-onset progressive HL.[4,5] The progression of HL in *Bth*-heterozygous mice ($Tmc1^{Bth/+}$) is reflected by degeneration of cochlear inner hair cells (IHCs) in a base-to-apex gradient (Figure 1A). Outer hair cells (OHCs) remain intact in a middle-to-apical region for at least the first 20 weeks of life.[6] Using an artificial microRNA (miRNA) carried in an adeno-associated virus (AAV) vector, we showed that selective suppression of the mutant *Tmc1* allele prevented HL as measured by auditory brainstem response (ABR) audiometry, and prolonged IHC survival as documented by immunohistochemistry (Figure 1B).[7] Other reports have also described successful auditory and/or balance restoration following intra-cochlear gene therapy in neonatal mouse models of genetic deafness.[7–18] These outcomes represent important advances; however, the neonatal murine inner ear is only partially developed and undergoes structural maturation until the onset of hearing at post-natal day (P) 14 and P15.[19] At P1–P2, it is temporally equivalent to the human cochlea prior to 26 weeks gestational age,[20] suggesting that translation of neonatal murine studies to human subjects would require *in utero* intervention.

Studies in mature animals are needed to assess the effect of gene therapy in the fully developed organ of Corti; however, delivering gene therapy to mice after the first post-natal week has been precluded by ossification of the bony labyrinth.[21] The murine bony labyrinth encases the membranous labyrinth and defines a non-expandable fluid-filled space of ~0.81 μL (0.62 μL of endolymph and 0.19 μL of perilymph).[22] Introducing more volume into this space is difficult and as a result, rates of hair cell transduction are low and the risk for iatrogenically induced HL is high.[23,24] To address this challenge, we developed a surgical approach in which round window membrane injection is combined with semi-circular canal fenestration (RWM+CF approach).[24] Canal fenestration adds an egress for fluid, making it possible to inject 1.0 μL of a therapeutic into the mature inner ear while preserving hearing. Herein, we

Received 31 August 2018; accepted 27 December 2018;
https://doi.org/10.1016/j.ymthe.2018.12.014.

Correspondence: Richard J.H. Smith, Department of Otolaryngology-Head and Neck Surgery, Carver College of Medicine, University of Iowa, 285 Newton Road, 5270 CBRB, Iowa City, IA 52242, USA.
E-mail: richard-smith@uiowa.edu

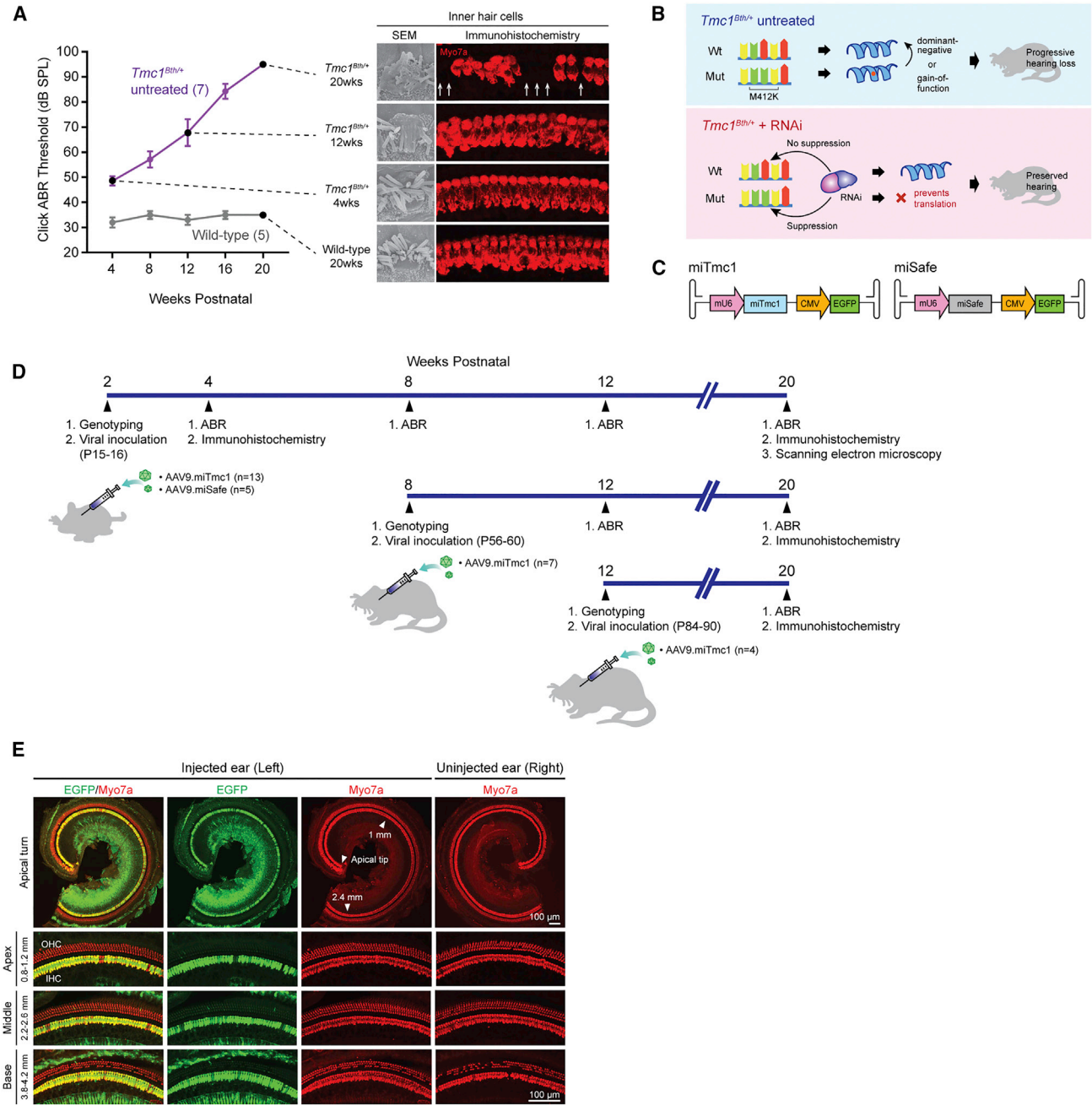

Figure 1. Overview of Therapeutic Concepts, Experimental Timeline, Progression of Hearing Loss, and Underlying Cochlear Morphology in *Tmc1*$^{Bth/+}$ Mice

Cochlear transgene delivery in *Tmc1*$^{Bth/+}$ mice shows robust transduction of IHCs. (A) Click-evoked ABR thresholds in wild-type and *Tmc1*$^{Bth/+}$ mice from 4 to 20 weeks with representative IHC images of scanning electron microscopy and immunohistochemistry at the indicated time points. Arrows indicate IHC loss; disorganized and fused stereocilia bundles increase over time on scanning electron microscopy. (B) Schematic overview with and without RNAi-mediated gene silencing in *Tmc1*$^{Bth/+}$ mice. (C) Transgene constructs. Dual-promoter viral insert with the U6 promoter driving miTmc miRNA or miSafe and the CMV promoter driving EGFP. (D) Experimental timeline with delivery of miRNAs at three different time points (P15–P16, P56–P60, and P84–P90). Outcomes followed by ABR, immunohistochemistry, and scanning electron microscopy. (E) Cochleae harvested 14 days after AAV9.miTmc1 RWM+CF injection in 2-week-old *Tmc1*$^{Bth/+}$ mice. Representative low-magnification images of whole-mount apical turns and high-magnification images of regions along the cochlea duct 0.8–1.2 mm (apex), 2.2–2.6 mm (middle), and 3.8–4.2 mm (base) from the apical tip.

report the first study to use gene therapy to treat progressive HL in mature *Tmc1*$^{Bth/+}$ mice.

RESULTS

AAV Vector Injection Using the RWM+CF Approach Transduces IHCs in the Mature *Tmc1*$^{Bth/+}$ Cochlea

A previously designed artificial miRNA-miTmc1 selectively suppresses expression of the mutant *Tmc1* allele and was used for these studies.[7] Using AAV2/9 carrying a dual transgene cassette of mouse U6 (mU6)-driven miTmc1 and downstream cytomegalovirus (CMV)-driven EGFP (AAV2/9.mU6.miTmc1.CMV.EGFP [AAV9.miTmc1, 3.30 × 10^{13} vg/mL]) (Figure 1C), we assessed transduction in *Tmc1*$^{Bth/+}$ mice by injecting the left ear at P15–P16 using the RWM+CF approach. Two weeks later, both ears were harvested and cochlear EGFP expression was quantitated in whole-mount preparations (Figure 1D). Transduction localized primarily to IHCs with a transduction efficiency of nearly 100% in all turns of the cochlea (apex [0.8–1.2 mm from apex tip]: 98.26% ± 0.54%; middle [2.2–2.6 mm from apex tip]: 100% ± 0.00%; and base [3.8–4.2 mm from apex tip]: 100% ± 0.00% (±SEM; n = 4; Figure 1E). Auditory thresholds as measured by ABR in injected and non-injected ears were comparable (Figure 2A). These results show that microinjection of AAV2/9 using the RWM+CF approach permits robust transduction of IHCs in the mature inner ear without damaging the organ of Corti.

AAV Transduction, Exogenous miRNAs, and EGFP Expression Do Not Cause Long-Term Hearing Impairment in Wild-Type Inner Ears

To exclude the possibility that AAV transduction, exogenous miRNAs, and/or EGFP expression cause oto-toxicity over time, we injected AAV9.miTmc1 into wild-type mice and followed these animals by ABR at 4-week intervals for 20 weeks and histology at the conclusion of the study. In injected ears relative to uninjected contralateral ears, we observed similar auditory thresholds across all frequencies and similar click-evoked peak 1 (P1) amplitudes and latencies (Figure S1A). Cochlear and vestibular whole mounts showed robust EGFP expression in cochlear IHCs and saccular hair cells (HCs) without HC loss (Figures S1B, S1C, S2A, and S2C). Collectively, these findings show that delivery of AAV9.miTmc1 into the mature inner ear does not cause HL and that expression of EGFP is stable for at least 18 weeks.

Allele-Specific Suppression Slows Hearing Impairment in Mature *Tmc1*$^{Bth/+}$ Mice

Tmc1$^{Bth/+}$ mice exhibit progressive HL, which by 16 weeks of age is severe to profound (Figure 1A). To evaluate the effect of allele-specific suppression mediated by RNAi, we injected P15–P16 *Tmc1*$^{Bth/+}$ mice with either AAV9.miTmc1 or AAV9.miSafe (AAV2/9.mU6.miSafe.CMV.EGFP) (3.90 × 10^{13} vg/mL) as a control (Figures 1C and 1D). Auditory function was measured as click and tone-burst evoked ABRs in four groups of mice: (1) wild-type littermates, (2) *Tmc1*$^{Bth/+}$ uninjected, (3) *Tmc1*$^{Bth/+}$+AAV9.miTmc1, and (4) *Tmc1*$^{Bth/+}$+AAV9.miSafe. The expected deterioration of hearing was documented in *Tmc1*$^{Bth/+}$ uninjected control animals, which by 16 weeks of age had severe-to-profound HL (Figure 2A). The injected left ears of *Tmc1*$^{Bth/+}$+AAV9.miSafe mice also had severe-to-profound levels of HL (Figure S2A). These results demonstrate that during the study period, neither the viral inoculation procedure nor the vector itself alters the expected degree of auditory dysfunction.

In the injected left ears of the *Tmc1*$^{Bth/+}$+AAV9.miTmc1 mice, hearing preservation was observed. By 8–12 weeks of age, the rate of HL was significantly reduced in treated as compared with untreated ears (Figure 2A). From 16 to 20 weeks of age, the mean difference in click-evoked ABR thresholds between treated and untreated ears was 25–30 dB sound pressure level (SPL). In the two best-performing *Tmc1*$^{Bth/+}$+AAV9.miTmc1 mice, hearing thresholds remained ∼50 dB better than in untreated *Tmc1*$^{Bth/+}$ mice (Figures 2A and 2F). Baseline hearing in *Tmc1*$^{Bth/+}$-treated animals was ∼10–15 dB worse than in wild-type mice at 4 weeks. Figure 2B shows representative ABR waveforms for each treatment group in response to click stimuli at 20 weeks. Uninjected ears lacked responses at any SPL. In contrast, ABR thresholds in AAV9.miTmc1 ears were recorded at 55 dB. These data demonstrate that miRNA-based gene therapy at P15–P16 significantly delays HL progression in *Tmc1*$^{Bth/+}$ mice.

Frequency-specific effects were measured with tone-burst ABRs (Figure 2C). Four-week-old *TmcF1*$^{Bth/+}$ untreated mice showed abnormal or absent hearing at 16 and 32 kHz, consistent with previous reports (Figure 2C, 4 weeks).[3,7,25] At 8 kHz, ABR responses were recordable until ∼12 weeks of age. In *Tmc1*$^{Bth/+}$+AAV9.miTmc1-treated mice, some degree of hearing was preserved at 8 kHz until 16 weeks of age, although a protective effect was not observed at 16 and 32 kHz at any time point (Figure 2C).

Defining the Temporal Window for Gene Therapy in *Tmc1*$^{Bth/+}$ Mice

To determine whether there is a temporal window for intervention, we treated P56–P60 and P84–P90 mice and measured click-evoked ABRs up to 20 weeks of age in (1) *Tmc1*$^{Bth/+}$ uninjected mice, (2) *Tmc1*$^{Bth/+}$+AAV9.miTmc1 mice treated at P56–P60, and (3) *Tmc1*$^{Bth/+}$+AAV9.miTmc1 mice treated at P84–P90 (Figure 1D).

Differences in auditory thresholds between untreated and treated ears in the P56–P60 treatment group became statistically significant at 12 weeks. From 16 to 20 weeks of age, the mean difference in ABR thresholds remained significant at 20–25 dB SPL (Figure 2D). Treatment at P84–P90 did not provide any hearing preservation, and in these mice hearing deterioration in treated and untreated ears was identical (Figure 2E). There appeared to be a mild protective effect on hearing as measured by tone-burst ABRs in mice treated at P56–P60, although the differences between untreated and treated ears at P56–P60 and P84–P90 were not significant at any time points (Figure S3).

To determine the effect of age at treatment, we measured hearing impairment as the intra-aural difference in ABR thresholds in

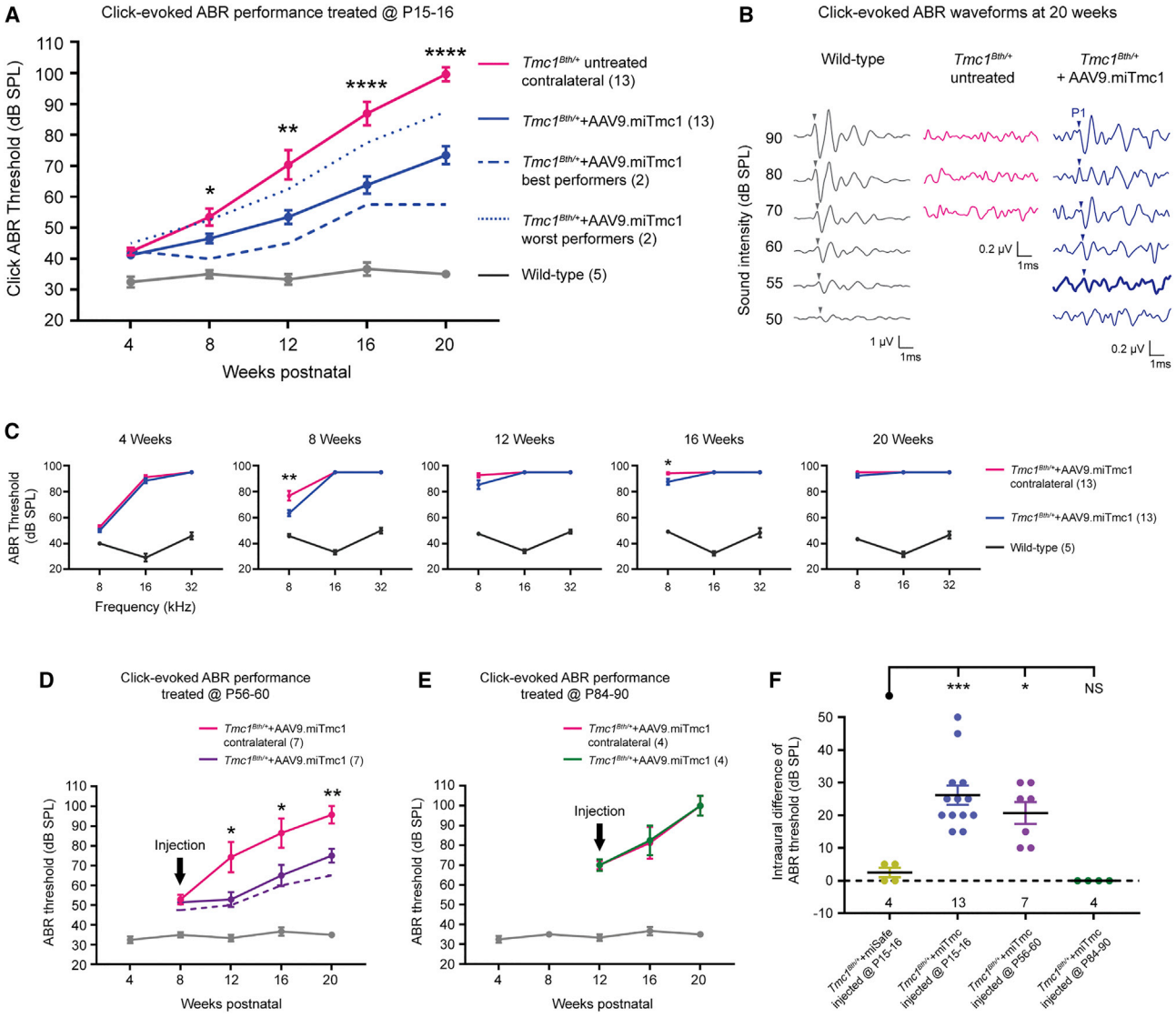

Figure 2. Targeted Allele Suppression Using miRNA-Based Gene Therapy Slows Progression of Hearing Loss in *Tmc1*$^{Bth/+}$ Mice

(A) Click ABR thresholds recorded longitudinally from 4 to 20 weeks in wild-type, *Tmc1*$^{Bth/+}$ untreated contralateral, and *Tmc1*$^{Bth/+}$+AAV9.miTmc1 P15–P16 treated ears. The two best-performing *Tmc1*$^{Bth/+}$+AAV9.miTmc1 animals are shown as dashed blue line. Data are means ± SEM. Statistical analysis by Student's t test. ****p < 0.0001; **p < 0.01; *p < 0.05. (B) Representative click-evoked ABR traces of 20-week-old mice recorded from wild-type, non-injected *Tmc1*$^{Bth/+}$ contralateral and *Tmc1*$^{Bth/+}$+AAV9.miTmc1 P15–P16 treated ears. Positive peaks 1 are indicated by arrowheads. Bold lines represent the detected thresholds. Non-injected *Tmc1*$^{Bth/+}$ contralateral ears show no ABR response at the sound levels tested. (C) Tone-burst ABR thresholds at 4, 8, 12, 16, and 20 weeks in wild-type, *Tmc1*$^{Bth/+}$ untreated contralateral and *Tmc1*$^{Bth/+}$+AAV9.miTmc1 P15–P16 treated ears. Data are means ± SEM. Statistical analysis by Student's t test: **p < 0.01; *p < 0.05. (D and E) Click ABR thresholds recorded longitudinally from 8 to 20 weeks in wild-type, *Tmc1*$^{Bth/+}$ untreated contralateral, and *Tmc1*$^{Bth/+}$+AAV9.miTmc1 ears treated at P56–P60 (D) and P84–P90 (E). The black arrow depicts the time point of injection. The two best-performing *Tmc1*$^{Bth/+}$+AAV9.miTmc1 animals treated at P56–P60 are shown as a dashed purple line (D). Data are means ± SEM. Statistical analysis by Student's t test: **p < 0.01; *p < 0.05. (F) ABR thresholds depicted as intraaural differences between *Tmc1*$^{Bth/+}$+AAV9.miSafe and *Tmc1*$^{Bth/+}$+AAV9.miTmc1 ears treated at P15–P16, P56–P60, and P84–P90. Statistical analysis by one-way ANOVA: ***p < 0.001; *p < 0.05. NS, statistically not significant. See also Figure S1.

mice treated at different time points. When compared with *Tmc1*$^{Bth/+}$+AAV9.miSafe as a control, mice treated with *Tmc1*$^{Bth/+}$+AAV9.miTmc1 at P15–P16 and P56–P60 demonstrated significant intra-aural differences in ABR thresholds. However, there were no differences in intra-aural thresholds at P84–P90 or when *Tmc1*$^{Bth/+}$+AAV9.miSafe was used (Figure 2F). These data demonstrate that although targeted allele suppression mediated by miRNA-based therapy is feasible in mature *Tmc1*$^{Bth/+}$ mice, the effect of therapy is impacted by the age of the treated animals.

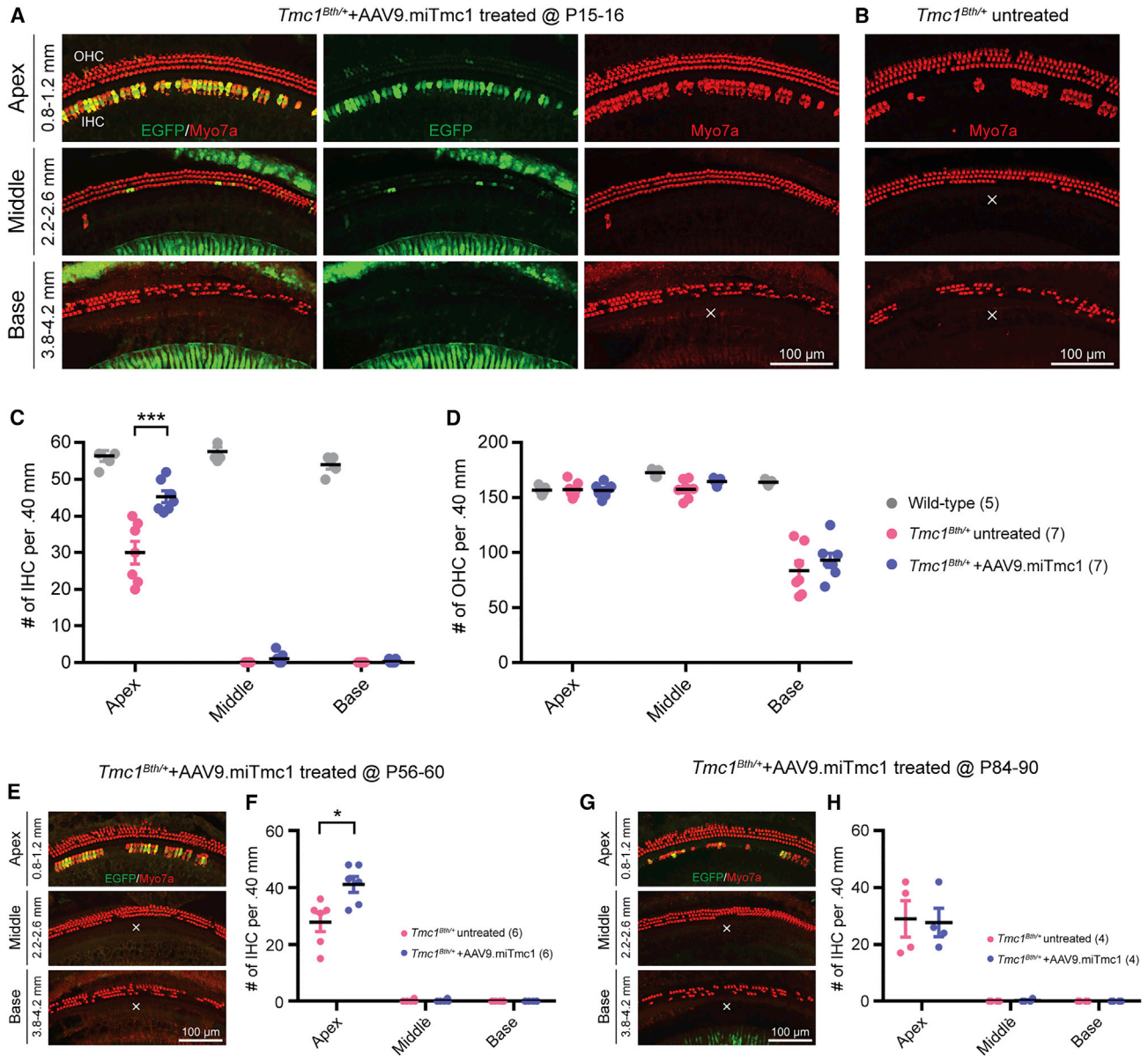

Figure 3. Targeted Allele Suppression Using miRNA-Based Gene Therapy Improves IHC Survival in *Tmc1*$^{Bth/+}$ Mice

(A, B, E, and G) Cochlear whole-mount images of *Tmc1*$^{Bth/+}$+AAV9.miTmc1 ears injected at P15–P16 (A), P56–P60 (E), and P84–P90 (G) compared with *Tmc1*$^{Bth/+}$ untreated contralateral ears. (B) Representative images of each turn of the cochlea. Distance from the apical tip is indicated. The white X shows the area devoid of IHCs. (C, D, F, and H) Quantitative comparison of IHC (C) and OHC (D) survival in wild-type, *Tmc1*$^{Bth/+}$ untreated contralateral, and *Tmc1*$^{Bth/+}$+AAV9.miTmc1 P15–16 treated ears, and IHC survival in *Tmc1*$^{Bth/+}$+AAV9.miTmc1 P56-60 treated (F) and P84–P90 treated (H) ears as compared with *Tmc1*$^{Bth/+}$ untreated contralateral ears. Hair cell counting in 400-µm segments across different regions of the cochlea (apex, middle, and base) at 20 weeks. Data are means ± SEM. Statistical analysis by Student's t test: ***$p < 0.001$; *$p < 0.05$.

Gene Therapy Alters Hair Cell Degeneration in Mature *Tmc1*$^{Bth/+}$ Mice

Histology at 20 weeks of age demonstrated no evidence of inflammation or tissue damage in the treated ears. Hair cells were labeled using an anti-Myo7a antibody and counted in 400-µm sections to quantitate the effect of miTmc1 on hair cell survival in (1) wild-type littermates, (2) *Tmc1*$^{Bth/+}$ uninjected contralateral ears, (3) *Tmc1*$^{Bth/+}$+AAV9.miTmc1 ears treated at P15–P16, (4) *Tmc1*$^{Bth/+}$+AAV9.miSafe ears treated at P15–P16, (5) *Tmc1*$^{Bth/+}$+AAV9.miTmc1 ears treated at P56–P60, and (6) *Tmc1*$^{Bth/+}$+AAV9.miTmc1 ears treated at P84–P90. In untreated *Tmc1*$^{Bth/+}$ mice, OHC loss was limited to the basal region, whereas IHC loss was 100% in the basal and middle turns and ~40% in the apical turn, consistent with other reports (Figures 3B–3D).[6] No obvious OHC or IHC loss was seen in

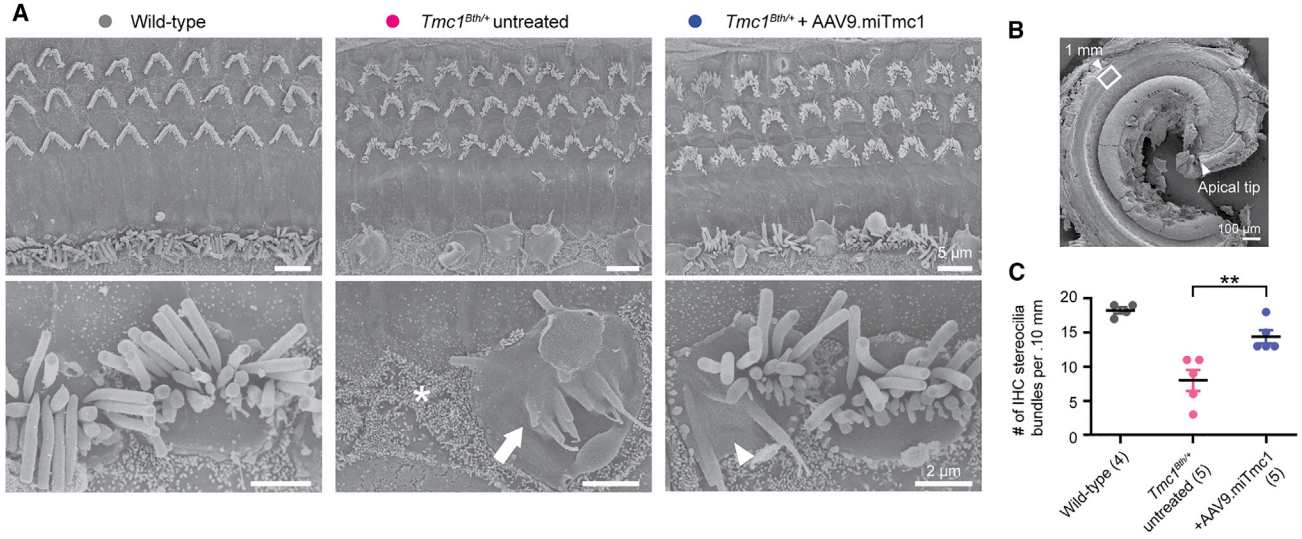

Figure 4. Targeted Allele Suppression Using miRNA-Based Gene Therapy Rescues IHC Bundle Morphology in *Tmc1*$^{Bth/+}$ Mice

(A) Representative scanning electron microscopy images (top) of the organ of Corti of wild-type, *Tmc1*$^{Bth/+}$ untreated contralateral, and *Tmc1*$^{Bth/+}$+AAV9.miTmc1 P15–P16 treated ears. The apical region (1.0 mm from the apical tip) of the organ of Corti was imaged at 20 weeks. High-magnification images (bottom) represent IHC hair bundles. Asterisk, arrow, and arrowheads indicate IHC loss and fully and partially fused stereocilia, respectively. (B) Low-magnification scanning electron micrograph illustrating the cochlea apical turn. The white box represents 1.0 mm from the apical turn and is represented in (A). (C) Quantitative comparison of hair cell counts per 100 µm of the apical region of the cochlea using scanning electron microscopy images in wild-type, *Tmc1*$^{Bth/+}$ untreated contralateral, and *Tmc1*$^{Bth/+}$+AAV9.miTmc1 P15–P16 treated ears. Data are means ± SEM. Statistical analysis by Student's t test: **p < 0.01.

20-week-old wild-type control animals (Figures 3D and 3E; Figures S1B and S1C).

Frequency mapping in the murine cochlea demarks the region corresponding to clicks and 8-kHz tone bursts as ~0.8–1.2 mm from the apex tip. Counting hair cells in this region in P15–P16 treated and contralateral untreated ears showed significantly higher numbers of surviving IHCs on the treated side (Figures 3A–3C), consistent with improved auditory function. IHC degeneration in AAV2/9.miSafe ears was indistinguishable from untreated ears (Figures S2B and S2C). In the mid-to-basal regions of the cochleae (16–32 kHz), no IHCs were observed in all groups (Figures 3A–3C; Figures S2B and S2C). OHC survival was comparable in treated and non-treated animals (Figure 3D; Figure S2D).

In P56–P60 treated ears, we observed statistically better IHC survival in apical turns as compared with untreated ears (Figures 3E and 3F). At P84–P90, there was no difference between treated and untreated ears (Figures 3G and 3H). These data demonstrate that targeted allele suppression with miRNA in P56–P60 *Tmc1*$^{Bth/+}$ mice (~8 weeks) can alter the course of IHC degeneration in the apical, but not the mid- or basal, cochleae.

We also studied whole mounts of vestibular saccule epithelia. In both treated and untreated *Tmc1*$^{Bth/+}$ mice, no hair cell loss was seen (Figures S4B and S4C), consistent with the observation that *Tmc1* null mice have normal vestibular function.[26] Treatment was associated with robust EGFP expression in the sensory epithelia of the saccule (Figures S4B and S4C), indicating safe transduction following the RWM+CF approach for at least 20 weeks.

miRNA-Based Gene Therapy Preserves IHC Stereocilia Morphology in *Tmc1*$^{Bth/+}$ Mice

We assessed IHC stereocilia morphology by scanning electron microscopy. In wild-type mice at 20 weeks of age, IHCs were preserved and hair bundle morphology was normal (Figure 4A). In untreated *Tmc1*$^{Bth/+}$ mice, we observed fusion of IHC stereocilia in the basal and middle cochlear regions by 4 weeks of age. By 8 weeks of age, the majority of IHCs had lost hair bundles, a finding consistent with other reports.[3,25] In the apical region, signs of IHC degeneration were apparent at ~12 weeks of age and progressively worsened thereafter. Although bundle disruption in OHCs was seen at the basal region from 2 weeks of age, most OHCs were still present in the apical region at 20 weeks. Overall, bundle disruption was more pronounced in IHCs as compared with OHCs and progressed from the base to the apex, as reported (Figure S5).[25]

Scanning electron microscopy images in *Tmc1*$^{Bth/+}$ untreated contralateral ears showed loss and severe disorganization of IHC hair bundles with fused stereocilia in the apical region (Figures 4A and 4B). In contrast, treated ears had significantly more IHC bundles (Figure 4C). Although the bundles in most of the IHCs and OHCs were still abnormal and disorganized, there were some IHC bundles with relatively normal morphology in treated ears, which were never seen in untreated ears (Figure 4A). These data indicate that targeted allele suppression in *Tmc1*$^{Bth/+}$ mice protects

IHC stereocilia bundles from degeneration when measured at 20 weeks of age.

DISCUSSION

In this study, we present the first successful application of cochlear gene therapy in an adult mouse model of progressive human deafness and demonstrate that RNAi can decrease the rate of progression of HL in the mature *Bth* mouse, a model of human *TMC1* deafness (DFNA36 [MIM: 606705]). Using an artificial miRNA carried in AAV2/9 vector and delivered at P15–P16, P56–P60, or P84–P90 to $Tmc1^{Bth/+}$ mice, we show that auditory impairment is reduced by up to 50 dB for over 20 weeks (the duration of the study) in animals treated at P15–P16, by up to 30 dB in animals treated at P56–P60, and not at all in animals treated at P84–P90. Treatment at P15–P16 and P56–P60 slows stereocilia bundle degeneration and prolongs survival of IHCs, the anatomic correlates of the improved auditory function. Absence of an effect at P84–P90 demonstrates that while targeted allele suppression mediated by miRNA-based therapy is feasible in mature $Tmc1^{Bth/+}$ mice, the effect of therapy is impacted by the age of the treated animals.

Auditory thresholds in RNAi-treated $Tmc1^{Bth/+}$ mice were elevated relative to those in wild-type mice, indicating incomplete rescue of auditory function. Although low transduction efficiency following viral delivery has been a common explanation for variable hearing outcomes following cochlear gene therapy,[7,9,11,12,14,15,27] we noted that a single injection of AAV2/9 at P15–P16 using the RWM+CF approach resulted in virtually complete transduction of all IHCs throughout the cochlea. Thus, other factors may have impacted our results, including degree of allele suppression and ongoing, irreversible HC damage.

With respect to the first point, it may be germane that neither *in vivo* nor *in vitro* RNAi-mediated allele-specific suppression is complete,[7] suggesting that improved suppression of the mutant allele may offer greater preservation of hearing thresholds. Although off-target effects like saturation of RNAi machinery, passenger-strand-mediated silencing, seed-mediated silencing, and immunostimulation can impact outcome of RNAi therapies,[28] the miRNA we chose was selected to minimize off-target molecular changes at the hair cell level.[29] Consistent with this choice, in wild-type mice injected with miTmc1 at P15–P16, there was no evidence of HL or hair cell damage at 20 weeks in the presence of persistent and widespread expression of EGFP. These findings suggest that the off-target effects of miTmc1 are minimal and unlikely to contribute to HL.

Treatment at P56–P60 also offers a mild protective effect on hearing. The number of surviving IHCs in treated as compared with untreated ears was statistically greater and was similar to the results observed in P15–P16 treated mice. However, when treatment was delayed until P84–P90, there was no impact of therapy, defining a boundary somewhere between P56–P60 and P84–P90 before which $Tmc1^{Bth/+}$ mice must be treated if some degree of auditory decline is to be halted.

With respect to ongoing HC damage in $Tmc1^{Bth/+}$ mice, scanning electron microscopy data show that stereocilia bundles in the apical region are healthy until 8 weeks, but by 12 weeks are fused and degenerating, a morphological change that resembles the degeneration of HCs in many other murine models of genetic deafness.[25,30–35] Our results suggest that gene therapy in $Tmc1^{Bth/+}$ mice must be delivered prior to the onset of IHC degeneration. As compared with our results following treatment at P0–P2,[7] the extent of hearing preservation as measured by intra-aural differences in click-evoked ABR thresholds was similar in animals treated at P15–P16 and P56–P60 (22.8, 26.1, and 20.7 dB, respectively). Delivery after degeneration has started does not alter the progression of HL, implying that $Tmc1^{Bth/+}$ HL is potentially preventable, but not reversible. Once structural degeneration begins, gene therapy will not reverse this process.[12] One limitation of this study is that we analyzed only hair cell morphology. Further studies are required to assess the impact of RNAi on mechanosensory transduction.

Degeneration begins in the base as early as 2 weeks of age and spreads apically. We speculate that the degree of RNAi we achieve is inadequate to overcome the dominant-negative effect of the *Tmc1* M412K allele and/or that irreversible changes at the molecular level occur early. Both possibilities are consistent with our data, which show an inability to slow the progression of high frequencies of HL in spite of IHC transduction. Additional studies at the single-cell level may help to resolve the molecular basis for this limitation, potentially allowing us to refine RNAi-based gene therapy in this specific animal model. In P0–P2 $Tmc1^{Bth/+}$ mice treated with RNAi[7] or CRISPR-Cas9 genomic editing,[36] treatment slows both mid- to high-frequency and low-frequency HL, and improves IHC survival at the mid-basal turns of the cochlea, suggesting that early intervention may improve phenotypic rescue (Figure S6).[8,16] In human *TMC1* deafness (DFNA36), although HL is severe to profound by 60 years of age, its onset varies from 5 to 28 years.[4,5] Because deterioration of HL is much slower in humans than in $Tmc1^{Bth/+}$ mice, there may be a greater temporal window for successful therapeutic intervention, which could allow for rescue of the mid to high frequencies.

In summary, we show that RNAi-mediated targeted allele suppression slows progression of HL and improves IHC survival in mature $Tmc1^{Bth/+}$ mice. The temporal window for successful intervention lies somewhere between 8 and 12 weeks after birth. Treatment after 12 weeks has no impact on HL, and progression continues at a rate indistinguishable from untreated animals. These findings suggest that for *TMC1*-related deafness, the opportunity to intervene using RNAi is temporally defined and beyond a specific time point, and targeted allele suppression will have no effect. Whether these constraints are applicable to other types of gene therapy directed at correcting *TMC1*-related deafness, or whether other genetic forms of HL show gene-specific temporal windows for intervention is not known. Addressing these questions is highly relevant to the continued development of gene therapy as a habilitation option for human HL.

MATERIALS AND METHODS

Ethics Approvals

All experiments were approved by the University of Iowa Institutional Biosafety Committee (IBC; rDNA Committee; RDNA Approval Notice #100024) and the University of Iowa Institutional Animal Care and Use Committee (IACUC; Protocol #06061787), and were performed in accordance with the NIH *Guide for the Care and Use of Laboratory Animals*.

Mice

Mice were housed in a controlled temperature environment on a 12-h light-dark cycle. Food and water were provided *ad libitum*. Isogenic heterozygous Beethoven mice ($Tmc1^{Bth/+}$) maintained on a C3HeB/FeJ (C3H) background were obtained as a gift from Dr. Karen Steel.[3] Inbred wild-type C3H were obtained from the Jackson Laboratory. Crossbred homozygous $Tmc1^{Bth/Bth}$ mice were caged with wild-type C3H mice to generate heterozygous $Tmc1^{Bth/+}$ animals. Genotyping was done on DNA from tail-clip biopsies extracted using the Proteinase K method and amplified with forward (5′-CTAATCATAC CAAGGAAACATATGGAC-3′) and reverse (5′-TAGACTCACCT TGTTGTTAATCTCATC-3′) primers in a 20-μL volume containing 40 ng of DNA, 24 pmol of each primer and BioLase DNA polymerase (Bioline USA, Taunton, MA, USA) to generate a 376-bp amplification product in $Tmc1^{Bth/+}$ mice. Amplification conditions included an initial 5-min denaturation at 95°C followed by 35 step cycles of 1 min at 95°C, 1.5 min at 58°C, and 1.5 min at 72°C, with a final elongation of 5 min at 72°C. PCR products were purified and sequenced on an automated sequencer (ABI PRISM 3130xl genetic analyzer; Applied Biosystems, Foster City, CA).

Virus Production

AAV viral vectors were prepared by the Viral Vector Core at the University of Iowa as described previously.[37] AAV2/9 (abbreviated AAV9.miTmc1) carrying a dual transgene cassette of mU6-driven miRNA#16 targeting Met412Lys allele and downstream CMV-driven EGFP were generated as therapeutic vectors; AAV2/9 containing mU6-driven miSafe and downstream CMV-driven EGFP (abbreviated AAV9.miSafe) was prepared as a control vector as described previously.[7] Viral titers were AAV9.miTmc1 at 3.30×10^{13} vg/mL and AAV9.miSafe at 3.90×10^{13} vg/mL. Virus aliquots were stored at −80°C and thawed before use.

Animal Surgery

A round window membrane injection combined with canal fenestration (RWM+CF injection) was carried out as described previously.[24] Mice were anesthetized with an intraperitoneal injection of ketamine (100 mg/kg) and xylazine (10 mg/kg). Body temperature was maintained with a heating pad during the surgical procedure. The left post-auricular region was shaved and cleaned. Surgery was performed under an operating microscope. A post-auricular incision was made to access the temporal bone. The facial nerve was identified deep along the wall of the external auditory canal. After exposing the facial nerve and the sternocleidomastoid muscle (SCM), a portion of the muscle was divided to expose the cochlea bulla ventral to the facial nerve. The posterior semicircular canal (PSCC) was exposed dorsal to the cochlea bulla. A 0.5- to 1.0-mm diameter otologic drill (ANSPACH EMAX2 2 Plus System; DePuy, Raynham, MA, USA) was used to make a small hole in the cochlea bulla, which was then widened sufficiently with forceps to visualize the stapedial artery and the RWM. A hole was also drilled in the PSCC with a 0.5-mm diameter diamond drill; slow egress of perilymph confirmed a patent canalostomy.

After waiting 5–10 min for perilymph egress to abate, 1.0 μL of AAV vectors with 2.5% fast green dye (Sigma-Aldrich, St. Louis, MO, USA) was loaded into a borosilicate glass pipette (1.5-mm outer diameter [OD] × 0.86-mm inner diameter [ID]; Harvard Apparatus, Hollison, MA, USA) pulled with a Sutter P-97 micropipette puller to a final OD of ∼15 μm and affixed to an automated injection system pressured by compressed gas (Harvard Apparatus). Pipettes were manually controlled with a micropipette manipulator. The RWM was punctured gently in the center, and AAV was microinjected into the scala tympani for 5 min (30–40 nL per injection). Successful injections were confirmed by visualizing the efflux of green fluid from the PSCC canalostomy. After pulling out the pipette, the RWM niche was sealed quickly with a small plug of muscle to avoid leakage. The bony defect of the bulla and canal was sealed with small plugs of muscles and Vetbond tissue adhesive (3M, Maplewood, MN, USA). 6-0 absorbable polypropylene sutures and 6-0 nylon monofilament sutures were used to close the SCM and skin, respectively. Total surgical time ranged from 20 to 30 min for 2-week-old mice and from 50 to 60 min for 8- and 12-week-old mice. After all procedures, mice were placed on a heating pad for recovery and rubbed with bedding. Two-week-old mice were returned to their mothers. Pain was controlled with buprenorphine (0.05 mg/kg) and flunixin meglumine (2.5 mg/kg) for 3 days. Recovery was closely monitored daily for at least 5 days post-operatively. All animals were operated on by one surgeon (H.Y.).

Auditory Testing

ABRs were recorded as described previously.[24,38] All mice were anesthetized with an intraperitoneal injection of ketamine (100 mg/kg) and xylazine (10 mg/kg). All recordings were conducted from both ears of all animals on a heating pad using electrodes placed subcutaneously in the vertex and underneath the left or right ear. Clicks were square pulses 100 ms in duration, and tone bursts were 3 ms in length at distinct 8-, 16-, and 32 kHz frequencies. ABRs were measured with BioSigRZ (Tucker-Davis Technologies, Alachua, FL, USA) for both clicks and tone bursts, adjusting the stimulus levels in 5-dB increments between 25 and 100 dB SPLs in both ears. Electrical signals were averaged over 512 repetitions. ABR threshold was defined as the lowest sound level at which a reproducible waveform could be observed. For transduction efficiency analysis, ABRs were measured 2 weeks after the injection; for gene therapy experiments, 4-week intervals for 20 weeks. Responses from the contralateral ear, which did not undergo surgery, were used as controls.

Immunohistochemistry, Cell Counts, and Transduction Efficiency Analysis

All injected and non-injected cochleae were harvested after animals were sacrificed by CO_2 inhalation. Temporal bones were locally perfused and fixed in 4% paraformaldehyde for 2 h at 4°C, rinsed in PBS, and stored at 4°C in preparation for immunohistochemistry. Specimens were visualized with a dissection microscope and dissected for whole-mount analysis. In all of the cochlear and vestibular whole mounts, GFP was detected by its intrinsic fluorescence. Following infiltration using 0.3% Triton X-100 for 30 min and blocking with 5% normal goat serum for 1 h, tissues were incubated with rabbit polyclonal Myosin-VIIA antibody for hair cells (#25-6790; Proteus Biosciences, Ramona, CA, USA) diluted 1:200 in PBS for 1 h. Subsequently, fluorescence-labeled goat anti-rabbit immunoglobulin G (IgG) Alexa Fluor 568 (#A-11036; Thermo Fisher Scientific, Rockford, IL, USA) in 1:500 dilution was used as a secondary antibody for 30 min. Specimens were mounted in ProLong Diamond Antifade Mountant with DAPI (#P36965; Thermo Fisher Scientific) and observed with a Leica TCS SP8 confocal microscope (Leica Microsystems, Bannockburn, IL, USA). Cell counts and transduction efficiency analysis were performed as described previously.[24,38] z stack images of whole mounts were collected at 10×–20× on a Leica SP8 confocal microscope. Each turn of the cochlea was analyzed: 0.8–1.2 mm (apex), 2.2–2.6 mm (middle), and 3.8–4.2 mm (base) of the total length from the apical tip. The corresponding approximate frequencies are 8, 16, and 32 kHz, respectively.[39] Maximum intensity projections of z stacks were generated for each field of view, and images were prepared using LAS X (Leica Microsystems) to meet equal conditions. IHCs with positive EGFP and overlapping Myo7a were counted per 400-µm cochlear sections for each turn in each specimen with ImageJ Cell Counter (NIH Image). The total numbers of HCs and GFP-positive HCs were summed and converted to a percentage.

Scanning Electron Microscopy and Quantification of IHC Degeneration

Cochleae were prefixed with fixative solution containing 2.5% glutaraldehyde in 0.1 M sodium cacodylate buffer and 4% paraformaldehyde with 2 mM $CaCl_2$ for 1 h at 4°C, microdissected in the same buffer, and then postfixed with 1% OsO_4 in the same buffer for 1 h. Specimens were dehydrated in a graded ethanol series, critical-point dried in liquid CO_2, mounted on stubs, and sputter-coated with gold-palladium (10 mA, 90 s). Samples were examined using an S-4800 field-emission scanning electron microscope (Hitachi, Japan) operated at 3 kV. IHC degeneration was quantified by counting the number of normal hair bundles and the number of degenerating hair bundles per 100-µm sections in the apical region, 1.0 mm from the apex tip for each specimen as described previously.[25]

Statistical Analysis

Sample sizes are noted in the figure legends. Data are presented as means ± SEM as noted in the figure legends. Statistical analysis was performed using Prism 7 software package (GraphPad, San Diego, CA, USA). Two groups were compared using unpaired two-tailed Student's t test. For comparisons of more than two groups, one-way ANOVA was performed and followed by *post hoc* analysis with Bonferroni correction of pairwise group differences. $p < 0.05$ was considered statistically significant.

SUPPLEMENTAL INFORMATION

Supplemental Information includes six figures and can be found with this article online at https://doi.org/10.1016/j.ymthe.2018.12.014.

AUTHOR CONTRIBUTIONS

R.J.H.S. conceived of the study; H.Y., S.B.S., and R.J.H.S. designed research; H.Y. and S.B.S. performed research and analyzed data; S.B.S., P.T.R., and H.M. contributed microRNA; H.Y., S.B.S., and R.J.H.S. wrote the paper.

CONFLICTS OF INTEREST

The authors declare no competing interests.

ACKNOWLEDGMENTS

We thank Susan Stamnes (University of Iowa Gene Transfer Vector Core) for assistance and for providing the viral vectors. This project was supported by NIH/NIDCD grants T32 DC000040-17 (to S.B.S.) and R01 DC03544 (to R.J.H.S.), and an AAO-HNSF Resident Research Grant 2013 (to S.B.S.).

REFERENCES

1. Mohr, P.E., Feldman, J.J., and Dunbar, J.L. (2000). The societal costs of severe to profound hearing loss in the United States. Policy Anal. Brief H Ser. *2*, 1–4.
2. Shibata, S.B., and Raphael, Y. (2010). Future approaches for inner ear protection and repair. J. Commun. Disord. *43*, 295–310.
3. Vreugde, S., Erven, A., Kros, C.J., Marcotti, W., Fuchs, H., Kurima, K., Wilcox, E.R., Friedman, T.B., Griffith, A.J., Balling, R., et al. (2002). Beethoven, a mouse model for dominant, progressive hearing loss DFNA36. Nat. Genet. *30*, 257–258.
4. Wang, H., Wu, K., Guan, J., Yang, J., Xie, L., Xiong, F., Lan, L., Wang, D., and Wang, Q. (2018). Identification of four TMC1 variations in different Chinese families with hereditary hearing loss. Mol. Genet. Genomic Med. *6*, 504–513.
5. Zhao, Y., Wang, D., Zong, L., Zhao, F., Guan, L., Zhang, P., Shi, W., Lan, L., Wang, H., Li, Q., et al. (2014). A novel DFNA36 mutation in TMC1 orthologous to the Beethoven (Bth) mouse associated with autosomal dominant hearing loss in a Chinese family. PLoS ONE *9*, e97064.
6. Noguchi, Y., Kurima, K., Makishima, T., de Angelis, M.H., Fuchs, H., Frolenkov, G., Kitamura, K., and Griffith, A.J. (2006). Multiple quantitative trait loci modify cochlear hair cell degeneration in the Beethoven (Tmc1Bth) mouse model of progressive hearing loss DFNA36. Genetics *173*, 2111–2119.
7. Shibata, S.B., Ranum, P.T., Moteki, H., Pan, B., Goodwin, A.T., Goodman, S.S., Abbas, P.J., Holt, J.R., and Smith, R.J.H. (2016). RNA interference prevents autosomal-dominant hearing loss. Am. J. Hum. Genet. *98*, 1101–1113.
8. Akil, O., Seal, R.P., Burke, K., Wang, C., Alemi, A., During, M., Edwards, R.H., and Lustig, L.R. (2012). Restoration of hearing in the VGLUT3 knockout mouse using virally mediated gene therapy. Neuron *75*, 283–293.
9. Askew, C., Rochat, C., Pan, B., Asai, Y., Ahmed, H., Child, E., Schneider, B.L., Aebischer, P., and Holt, J.R. (2015). Tmc gene therapy restores auditory function in deaf mice. Sci. Transl. Med. *7*, 295ra108.
10. Chang, Q., Wang, J., Li, Q., Kim, Y., Zhou, B., Wang, Y., Li, H., and Lin, X. (2015). Virally mediated Kcnq1 gene replacement therapy in the immature scala media restores hearing in a mouse model of human Jervell and Lange-Nielsen deafness syndrome. EMBO Mol. Med. *7*, 1077–1086.
11. Emptoz, A., Michel, V., Lelli, A., Akil, O., Boutet de Monvel, J., Lahlou, G., Meyer, A., Dupont, T., Nouaille, S., Ey, E., et al. (2017). Local gene therapy durably restores

vestibular function in a mouse model of Usher syndrome type 1G. Proc. Natl. Acad. Sci. USA *114*, 9695–9700.

12. Geng, R., Omar, A., Gopal, S.R., Chen, D.H., Stepanyan, R., Basch, M.L., Dinculescu, A., Furness, D.N., Saperstein, D., Hauswirth, W., et al. (2017). Modeling and preventing progressive hearing loss in Usher syndrome III. Sci. Rep. *7*, 13480.
13. György, B., Sage, C., Indzhykulian, A.A., Scheffer, D.I., Brisson, A.R., Tan, S., Wu, X., Volak, A., Mu, D., Tamvakologos, P.I., et al. (2017). Rescue of hearing by gene delivery to inner-ear hair cells using exosome-associated AAV. Mol. Ther. *25*, 379–391.
14. Iizuka, T., Kamiya, K., Gotoh, S., Sugitani, Y., Suzuki, M., Noda, T., Minowa, O., and Ikeda, K. (2015). Perinatal Gjb2 gene transfer rescues hearing in a mouse model of hereditary deafness. Hum. Mol. Genet. *24*, 3651–3661.
15. Isgrig, K., Shteamer, J.W., Belyantseva, I.A., Drummond, M.C., Fitzgerald, T.S., Vijayakumar, S., Jones, S.M., Griffith, A.J., Friedman, T.B., Cunningham, L.L., and Chien, W.W. (2017). Gene therapy restores balance and auditory functions in a mouse model of Usher syndrome. Mol. Ther. *25*, 780–791.
16. Lentz, J.J., Jodelka, F.M., Hinrich, A.J., McCaffrey, K.E., Farris, H.E., Spalitta, M.J., Bazan, N.G., Duelli, D.M., Rigo, F., and Hastings, M.L. (2013). Rescue of hearing and vestibular function by antisense oligonucleotides in a mouse model of human deafness. Nat. Med. *19*, 345–350.
17. Pan, B., Askew, C., Galvin, A., Heman-Ackah, S., Asai, Y., Indzhykulian, A.A., Jodelka, F.M., Hastings, M.L., Lentz, J.J., Vandenberghe, L.H., et al. (2017). Gene therapy restores auditory and vestibular function in a mouse model of Usher syndrome type 1c. Nat. Biotechnol. *35*, 264–272.
18. Ponnath, A., Depreux, F.F., Jodelka, F.M., Rigo, F., Farris, H.E., Hastings, M.L., and Lentz, J.J. (2018). Rescue of outer hair cells with antisense oligonucleotides in Usher mice is dependent on age of treatment. J. Assoc. Res. Otolaryngol. *19*, 1–16.
19. Ehret, G. (1976). Development of absolute auditory thresholds in the house mouse (Mus musculus). J. Am. Audiol. Soc. *1*, 179–184.
20. Hall, J.W., 3rd (2000). Development of the ear and hearing. J. Perinatol. *20*, S12–S20.
21. Parker, M., Brugeaud, A., and Edge, A.S. (2010). Primary culture and plasmid electroporation of the murine organ of Corti. J. Vis. Exp. (36), 1685.
22. Thorne, M., Salt, A.N., DeMott, J.E., Henson, M.M., Henson, O.W., Jr., and Gewalt, S.L. (1999). Cochlear fluid space dimensions for six species derived from reconstructions of three-dimensional magnetic resonance images. Laryngoscope *109*, 1661–1668.
23. Chien, W.W., McDougald, D.S., Roy, S., Fitzgerald, T.S., and Cunningham, L.L. (2015). Cochlear gene transfer mediated by adeno-associated virus: comparison of two surgical approaches. Laryngoscope *125*, 2557–2564.
24. Yoshimura, H., Shibata, S.B., Ranum, P.T., and Smith, R.J.H. (2018). Enhanced viral-mediated cochlear gene delivery in adult mice by combining canal fenestration with round window membrane inoculation. Sci. Rep. *8*, 2980.
25. Marcotti, W., Erven, A., Johnson, S.L., Steel, K.P., and Kros, C.J. (2006). Tmc1 is necessary for normal functional maturation and survival of inner and outer hair cells in the mouse cochlea. J. Physiol. *574*, 677–698.
26. Kawashima, Y., Géléoc, G.S., Kurima, K., Labay, V., Lelli, A., Asai, Y., Makishima, T., Wu, D.K., Della Santina, C.C., Holt, J.R., and Griffith, A.J. (2011). Mechanotransduction in mouse inner ear hair cells requires transmembrane channel-like genes. J. Clin. Invest. *121*, 4796–4809.
27. Yu, Q., Wang, Y., Chang, Q., Wang, J., Gong, S., Li, H., and Lin, X. (2014). Virally expressed connexin26 restores gap junction function in the cochlea of conditional Gjb2 knockout mice. Gene Ther. *21*, 71–80.
28. Alagia, A., and Eritja, R. (2016). siRNA and RNAi optimization. Wiley Interdiscip. Rev. RNA *7*, 316–329.
29. Fellmann, C., and Lowe, S.W. (2014). Stable RNA interference rules for silencing. Nat. Cell Biol. *16*, 10–18.
30. Self, T., Sobe, T., Copeland, N.G., Jenkins, N.A., Avraham, K.B., and Steel, K.P. (1999). Role of myosin VI in the differentiation of cochlear hair cells. Dev. Biol. *214*, 331–341.
31. Hertzano, R., Shalit, E., Rzadzinska, A.K., Dror, A.A., Song, L., Ron, U., Tan, J.T., Shitrit, A.S., Fuchs, H., Hasson, T., et al. (2008). A Myo6 mutation destroys coordination between the myosin heads, revealing new functions of myosin VI in the stereocilia of mammalian inner ear hair cells. PLoS Genet. *4*, e1000207.
32. Sakaguchi, H., Tokita, J., Naoz, M., Bowen-Pope, D., Gov, N.S., and Kachar, B. (2008). Dynamic compartmentalization of protein tyrosine phosphatase receptor Q at the proximal end of stereocilia: implication of myosin VI-based transport. Cell Motil. Cytoskeleton *65*, 528–538.
33. Kitajiri, S., Sakamoto, T., Belyantseva, I.A., Goodyear, R.J., Stepanyan, R., Fujiwara, I., Bird, J.E., Riazuddin, S., Riazuddin, S., Ahmed, Z.M., et al. (2010). Actin-bundling protein TRIOBP forms resilient rootlets of hair cell stereocilia essential for hearing. Cell *141*, 786–798.
34. Ueyama, T., Sakaguchi, H., Nakamura, T., Goto, A., Morioka, S., Shimizu, A., Nakao, K., Hishikawa, Y., Ninoyu, Y., Kassai, H., et al. (2014). Maintenance of stereocilia and apical junctional complexes by Cdc42 in cochlear hair cells. J. Cell Sci. *127*, 2040–2052.
35. Ueyama, T., Ninoyu, Y., Nishio, S.Y., Miyoshi, T., Torii, H., Nishimura, K., Sugahara, K., Sakata, H., Thumkeo, D., Sakaguchi, H., et al. (2016). Constitutive activation of DIA1 (DIAPH1) via C-terminal truncation causes human sensorineural hearing loss. EMBO Mol. Med. *8*, 1310–1324.
36. Gao, X., Tao, Y., Lamas, V., Huang, M., Yeh, W.H., Pan, B., Hu, Y.J., Hu, J.H., Thompson, D.B., Shu, Y., et al. (2018). Treatment of autosomal dominant hearing loss by in vivo delivery of genome editing agents. Nature *553*, 217–221.
37. Yang, G.S., Schmidt, M., Yan, Z., Lindbloom, J.D., Harding, T.C., Donahue, B.A., Engelhardt, J.F., Kotin, R., and Davidson, B.L. (2002). Virus-mediated transduction of murine retina with adeno-associated virus: effects of viral capsid and genome size. J. Virol. *76*, 7651–7660.
38. Shibata, S.B., Yoshimura, H., Ranum, P.T., Goodwin, A.T., and Smith, R.J.H. (2017). Intravenous rAAV2/9 injection for murine cochlear gene delivery. Sci. Rep. *7*, 9609.
39. Viberg, A., and Canlon, B. (2004). The guide to plotting a cochleogram. Hear. Res. *197*, 1–10.

YMTHE, Volume *27*

Supplemental Information

Targeted Allele Suppression Prevents Progressive Hearing Loss in the Mature Murine Model of Human *TMC1* Deafness

Hidekane Yoshimura, Seiji B. Shibata, Paul T. Ranum, Hideaki Moteki, and Richard J.H. Smith

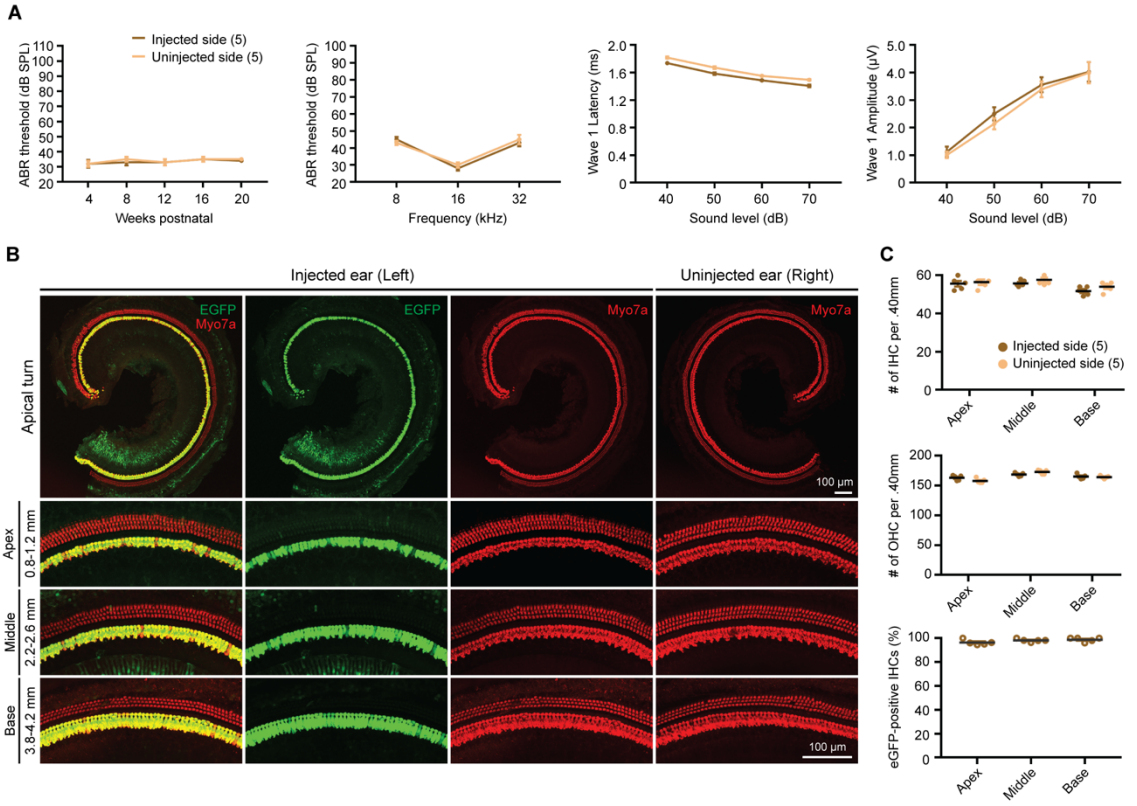

Figure S1. AAV9.miTmc delivery in wild-type cochlea showing robust long-term transduction without IHC and OHC losses and auditory dysfunction.

(A) Click-evoked ABR thresholds, Peak 1 latencies and amplitudes in AAV9.miTmc1-injected and uninjected ears in wild-type mice at 20 weeks of age. Data are means ± SEM.

(B) Cochlear whole-mount images of AAV9.miTmc1-injected and uninjected ears in wild-type mice sacrificed at 20 weeks. Representative low magnification images of whole-mount apical turns and high magnification images of each turn of the cochlea. Distance from the apical tip is indicated.

(C) Quantitative comparison of IHC and OHC survival and IHC transduction efficiency in AAV9.miTmc1-injected and uninjected ears in wild-type mice assessed in 400 μm segments across different regions of the cochlea (apex, middle and base). Data are means ± S.E.M.

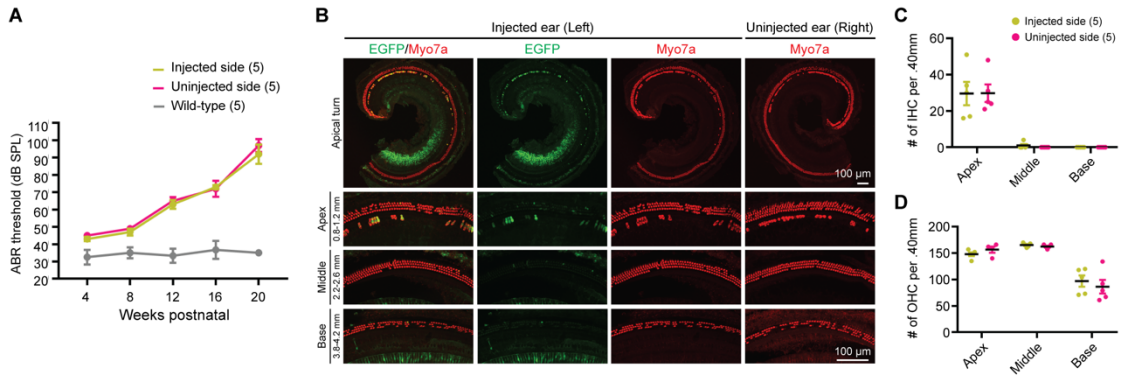

Figure S2. Auditory function and morphology of *Tmc1*$^{Bth/+}$+AAV9.miSafe injected ears at P15-16 are indistinguishable from that in *Tmc1*$^{Bth/+}$ untreated contralateral ears.

(A) Click ABR thresholds recorded longitudinally from 4 to 20 weeks in *Tmc1*$^{Bth/+}$ untreated contralateral, *Tmc1*$^{Bth/+}$+AAV9.miSafe animals.

(B) Cochlear whole-mount images of *Tmc1*$^{Bth/+}$+AAV9.miSafe treated at P15-16 and *Tmc1*$^{Bth/+}$ untreated contralateral animals sacrificed at 20 weeks. Representative low magnification images of apical turns and high magnification images of each turn of the cochlea. Distance from the apical tip is indicated.

(C, D) Quantitative comparison of IHC (C) and OHC (D) survival in *Tmc1*$^{Bth/+}$+AAV9.miSafe and *Tmc1*$^{Bth/+}$ untreated contralateral animals assessed in 400 µm segments across different regions of the cochlea (apex, middle and base). Data are means ± S.E.M.

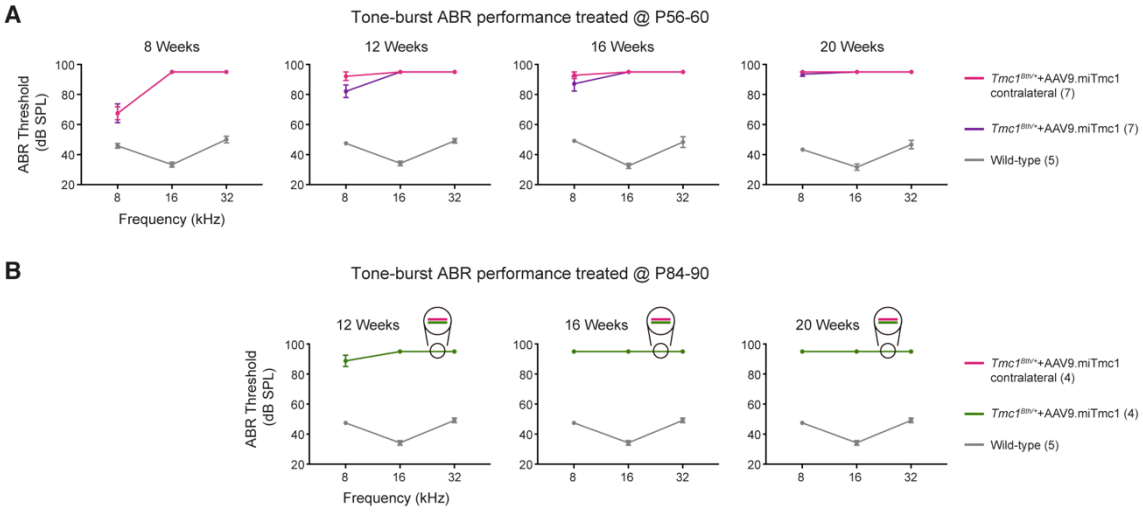

Figure S3. Frequency-specific ABR thresholds in the P56-60 and P84-90 treatment groups.

(A, B) Tone-burst ABRs at 8, 12, 16 and 20 weeks in wild-type mice, *Tmc1*$^{Bth/+}$ untreated contralateral ears, and *Tmc1*$^{Bth/+}$+AAV9.miTmc1 ears treated at P56-60 (A) and P84-90 (B). Data are means ± S.E.M.

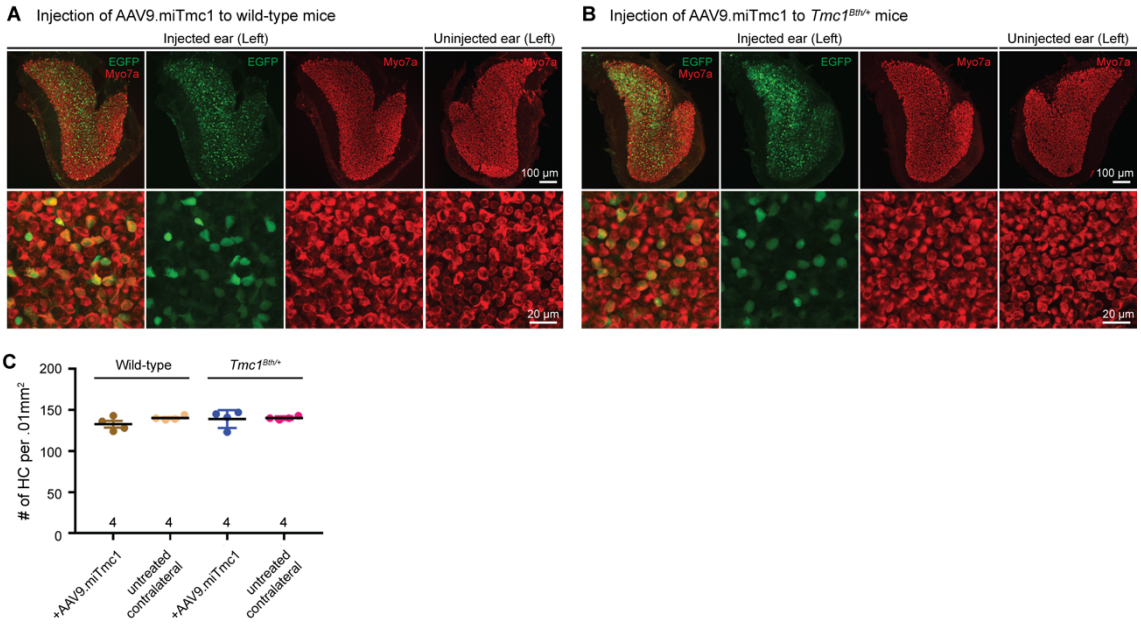

Figure S4. Hair cell survival in vestibular organ of wild-type and *Tmc1*$^{Bth/+}$ mice with and without cochlear transgene delivery

(A, B) Representative whole-mount images of the saccule of wild-type (A) and *Tmc1*$^{Bth/+}$ (B) mice sacrificed at 20 weeks of age. High-magnification images show transduced HCs (eGFP-positive; AAV transduction).

(C) Quantitative comparison of HC survival in wild-type and *Tmc1*$^{Bth/+}$ animals with and without the injection of AAV9.miTmc1.

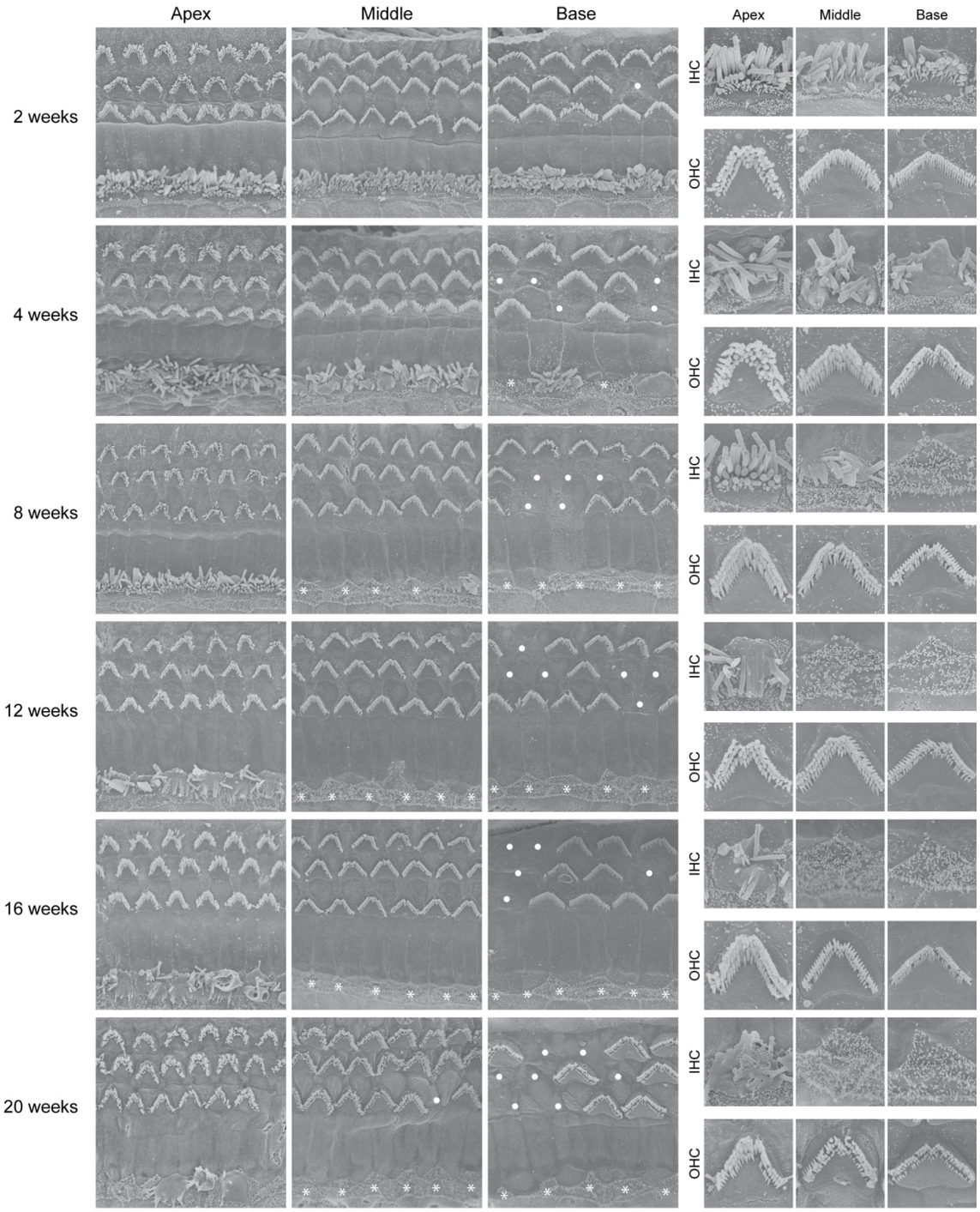

Figure S5. Scanning electron micrographs of *Tmc1*$^{Bth/+}$ mice of the organ of Corti.

Representative SEM images of the organ of Corti at the apex, middle and base obtained from untreated *Tmc1*$^{Bth/+}$ mice at 2, 4, 8, 12, 16 and 20 weeks of age. Asterisk and circles show IHC and OHC losses, respectively.

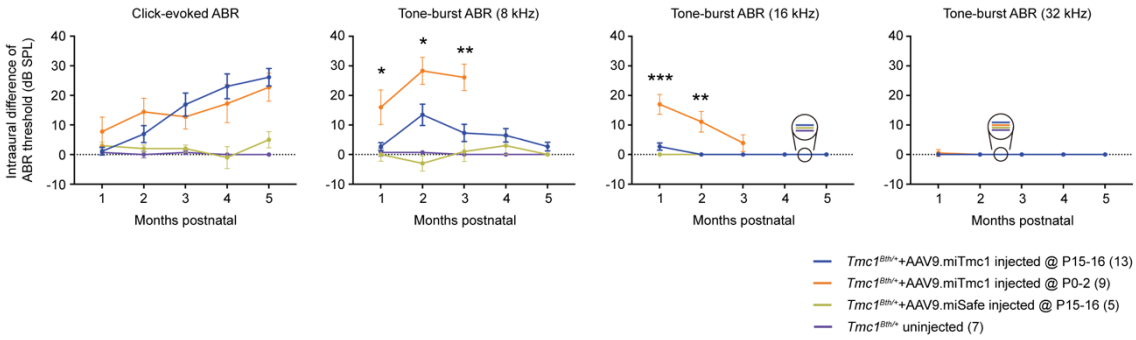

Figure S6. Click and tone-burst ABR thresholds.

Click and tone-burst ABR thresholds are shown as the intra-aural differences between ears in *Tmc1*$^{Bth/+}$+AAV9.miTmc1 animals injected at P0-2[7] and P15-16, *Tmc1*$^{Bth/+}$+AAV9.miSafe animals injected at P15-16, and in *Tmc1*$^{Bth/+}$ uninjected controls (***$P < 0.001$, **$P < 0.01$, *$P < 0.05$; Student's *t*-test). In the *Tmc1*$^{Bth/+}$+AAV9.miSafe animals and in *Tmc1*$^{Bth/+}$ uninjected controls, the is no difference in ABR thresholds between ears and hence the intra-aural difference is zero. The maximum intra-aural difference observed is seen in *Tmc1*$^{Bth/+}$+AAV9.miTmc1 animals injected at P0-2. These results show that phenotypic rescue as measured by tone-burst ABR is directly related to the age of the animal at the time of injection.